International Journal of Applied Research & Studies ISSN 2278 – 9480

Research Article

Experimental and FEA Prediction of Fatigue Life in Sheet Metal (IS 2062)

Authors

[1] Dr. Piyush Gohil, [2] Hemant N Panchal*, [3] Siddiqi Mahmud Sohail, [4] Devang V Mahant

Address for Correspondence:

[1] Assoc Professor, Dept. of Mechanical Engineering, Charotar Institute of Technology, Charotar Univ. of Science and Technology, Chnaga, Gujarat, India

[2, 3, 4] Assistant Professor, Mechanical Engineering Department, Parul Institute of Engineering & Technology (PIET), Vadodara,

***Abstract*— A practical fatigue analysis test set up was developed for predicting the life of sheet metal components. It was demonstrated that the predicted fatigue life for a sheet metal component can be performed with reasonable accuracy and efficiency by utilizing commercially available software. ANSYS and Fe-Safe, software were utilized as the finite element and fatigue life prediction solvers, respectively. Methodology consist of experimentally investigating the fatigue life of IS 2062 MS steel sheet metal component under constant amplitude loading. This approach was validated by comparing simulated life predictions using several stress-life and strain-life algorithms with the experimental results. Experimental setup was developed in house for testing of sheet metal components under fatigue. This work had demonstrated that a fatigue life methodology can be successfully utilized to predict the life of a sheet metal component in a practical manner.**

Keywords- Fatigue; Cantilever beam; Fatigue Testing machine; infrared sensors.

I. INTRODUCTION

In house development of simple and low cost Test rigs plays a major role for the up gradation of research and development at the Universities. This is a small step towards the sole purpose. A simple, low cost, high cycle fatigue test rig is design, developed and tested.

Berchem [1] has developed a fatigue testing machine in which we have tried to incorporate modifications which has made the machine more robust for the testing purpose. Modifications were regarding the reduction in the number of test specimens to be tested, usage of electronic device for cycle counting and adjustable chamber for the corrosion testing as it facilitates testing of composite components [2-7]

II. FATIGUE TESTING MACHINE SPECIFICATIONS

The Fatigue Test Rig designed to meet the following requirements:

- Capable of doing high-cycle fatigue testing.
- Displacement becomes the control parameter with controllable variable mean stress.
- Simultaneous testing of multiple specimens with easy accessibility.
- A robust cycle counting mechanism, recording number of cycles to failure for each individual test specimens.

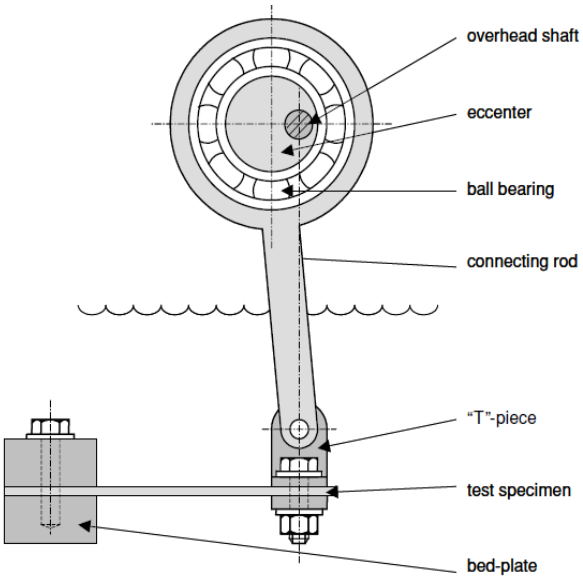

Figure 1. Schematic view of Fatigue testing principle [1]

III. DESIGN AND DEVLOPMENT OF FATIGUE TESTING MACHINE

Dimensions of the Fatigue Test Rig parts directly or indirectly depend on the size and shape of the test specimen.

Therefore first we shall decide upon the dimensions of the test specimen to be used.

A. Dimension determination of test specimen and eccentrics

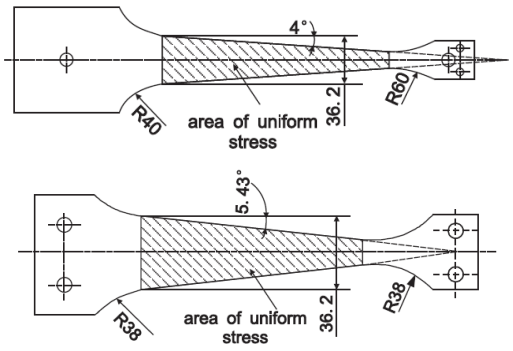

Figure 2. Stress distribution in the wedge shaped beam [Test specimen used by U.S.Naval Davy W. Tayloran Vessel Research Center (dimensions in mm)]

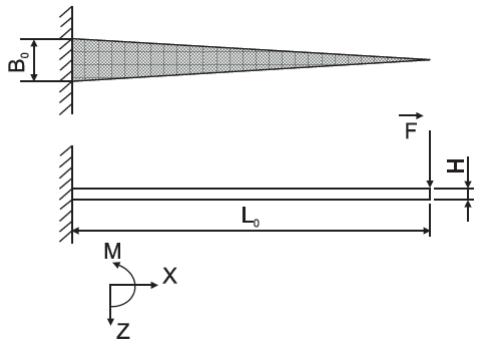

Figure 3. Schematic view of beam, with coordinates [Test specimen which used for corrosion fatigue testing ASM handbook recommended (dimensions in mm)][8]

Assuming that cross sections that are plane before bending remain plane after bending, and that the material follows Hooke's law, applying elastostatic theory of bending maximum stress at the surface is given as;

$$\sigma \max = \frac{M}{I} \cdot \frac{H}{2} \tag{1}$$

Here σ_{max} is the maximum stress, *M* the local bending moment, *H* the thickness of the beam, *I* the moment of inertia of the cross-sectional area.

As our specimen is a wedge shaped beam therefore the value of width *B* and thus the value of *I* depend on the position along X – axis.

$$B(x) = \frac{Bo}{Lo} \cdot \left(L_O - x\right) \tag{2}$$

Where,

B_o is the width at the base of the wedge shaped beam and L_o is the overall length.

Hence the moment of inertia equation becomes:

$$I(x) = \frac{B_O \cdot \left(L_O - x\right) \cdot H^3}{12 \cdot L_O} \tag{3}$$

The bending moment *M* also depends on the position along X – axis and is expressed as:

$$M_x = -F \cdot \left(L_O - x\right) \tag{4}$$

Where, *F* is the force applied at $x = L_o$, substituting equation (3) & (4) in equation (1) we have:

$$\sigma \max = -\frac{6 \cdot L_O \cdot F}{B_O \cdot H^2} \tag{5}$$

The maximum stress σ_{max} in a wedge-shaped beam therefore is independent of *x* and uniform over the whole length of the beam. It solely depends on the length L_o of the wedge, its thickness *H*, the width at the base B_o and the deflecting force *F* at its thin end.

B. Relation between the amount of deflection at the tip of a wedge-shaped beam and the maximum stress

The curve of the neutral plane in a bent beam is described by the 'differential equation of the deflection curve',

$$\frac{d^2 z}{dx^2} = -\frac{M}{E \cdot I} \tag{6}$$

Where *x* and *z* are points on *x* and *z* - axes, *M* is the local bending moment, *E* is the young's modulus and *I* is the moment of inertia of the cross-sectional area.

Substituting equations (3) & (4) in equation (6) we have:

$$\frac{d^2 z}{dx^2} = -\frac{F \cdot \left(L_O - x\right) \cdot 12 \cdot L_O}{E \cdot B_O \cdot \left(L_O - x\right) \cdot H^3} \tag{7}$$

$$\Leftrightarrow \frac{d^2 z}{dx^2} = \frac{12 \cdot F \cdot L_O}{E \cdot B_O \cdot H^3} \tag{8}$$

$$\Rightarrow \frac{dz}{dx} = \frac{12 \cdot F \cdot L_O}{E \cdot B_O \cdot H^3} \cdot x + C_1 \tag{9}$$

$$\Rightarrow z(x) = \frac{6 \cdot F \cdot L_O}{E \cdot B_O \cdot H^3} \cdot x^2 + C_1 x + C_2 \tag{10}$$

Where, C_1 and C_2 are integration constants.

The integration constants can be determined from the boundary conditions:

$\frac{dz}{dx}(o) = 0$ & $z(o) = 0$

This => $C_1 = 0$ & => $C_2 = 0$ substituting boundary condition values in equation (10) we have:

$$\Rightarrow z(x) = \frac{6 \cdot F \cdot L_O}{E \cdot B_O \cdot H^3} \cdot x^2 \tag{11}$$

Deflection *z(o)* at $x = L_o$, the tip of the wedge, where the connecting rod is acting:

$$z(o) = \frac{6 \cdot F \cdot L_O^3}{E \cdot BO \cdot H^3} \quad (12)$$

$$\Leftrightarrow F = \frac{Z_O \cdot E \cdot BO \cdot H^3}{6 \cdot L_O^3} \quad (13)$$

Substituting equation (13) into (5) we get:

$$\sigma \max = -\frac{z_o \cdot E \cdot H}{L_O^2} \quad (14)$$

The relation between the deflection *z(o)* at the tip and the maximum stress is linear as shown in figure 4

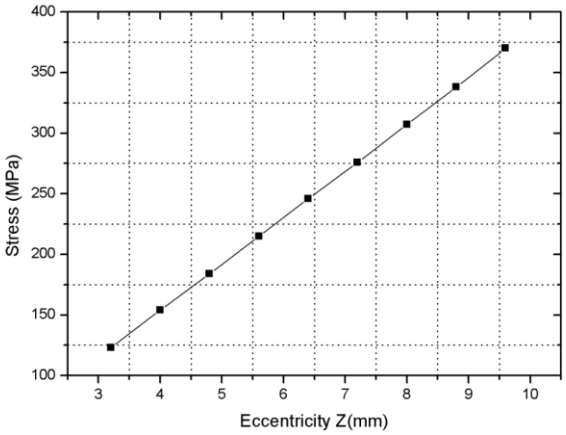

Figure 4 Fatigue test rig design and development with data acquisition system

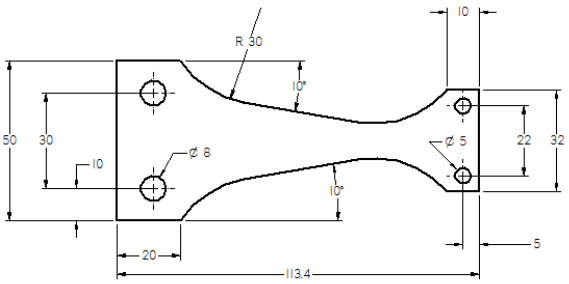

Figure 5 Drawing of final shape of specimen adopted for testing

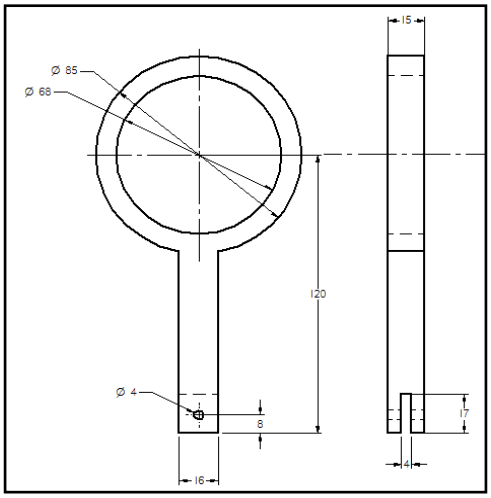

Figure 6 Drawing of connecting rod

Figure 5 to 8 shows the drawing of machine parts by software. Design details of various components of the fatigue testing machine are as follows:

- Whole of the setup was mounted on a plate, with two blocks supporting the shaft running in through two pedestal bearings. Motor used was of 0.5 HP induction type, running at 1440 rpm. Pulley size was selected so as to rotate the shaft at ~ 9 Hz. Power from motor to shaft was done by V-Belt.
- Shaft carried five eccentric wheels, which were secured on the shaft through grub screws. This provided flexibility in replacing the eccentrics as and when required.

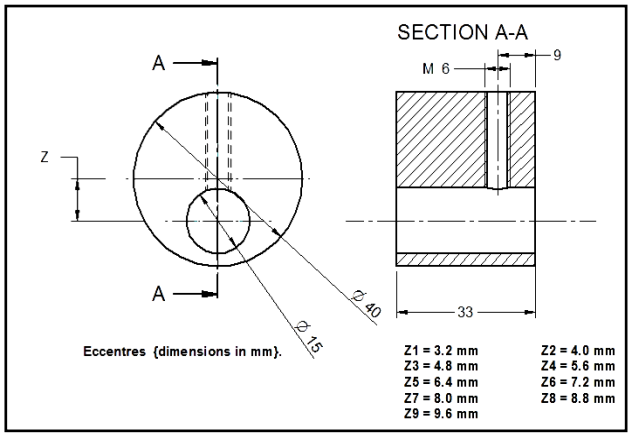

Figure 7 Drawing of eccentric

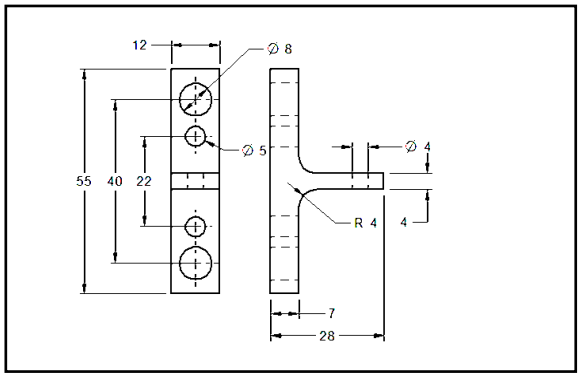

Figure 8 Drawing of T – Piece

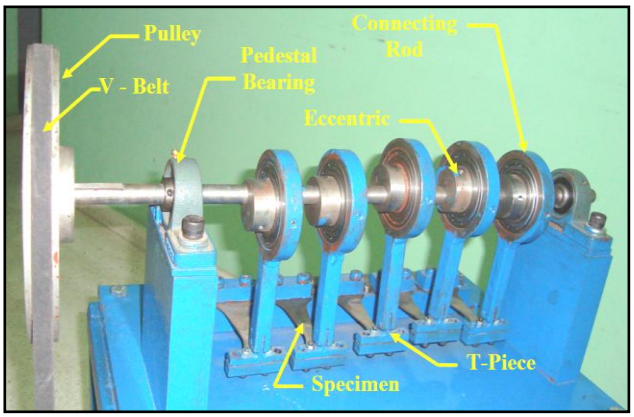

Figure 9 Experimental set up

Figure 9 shows the experimental set up along with specimens mounted in it. Cycle counting was done with the help of infrared sensors. A reflecting surface was mounted on the connecting rods and individual sensors counted the cycles. When the specimen failed the sensor disconnected the circuit as there was no reflection. Figure 10 shows the electrical connection of sensors with samples.

Testing procedure consisted of attaching first five eccentrics (3.2, 4.0, 4.8, 5.6 and 6.4) on the shaft and fixing five test specimens to the base plate. Machine was run till any of the specimens got fractured. Infrared sensors used gave the number of cycles.

As soon as any specimen frail, the counter as well as the machine stops working. The reading on the display gave the number of cycles to failure for that particular specimen.

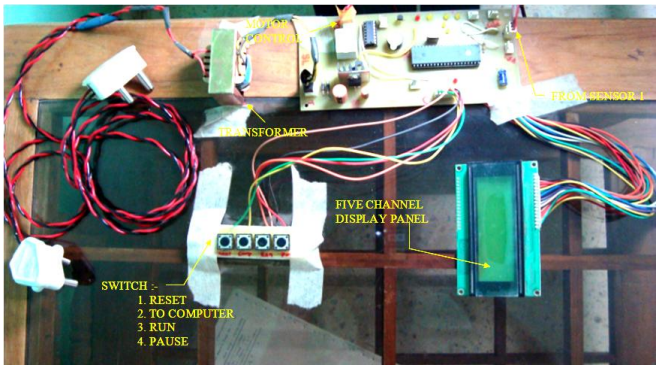

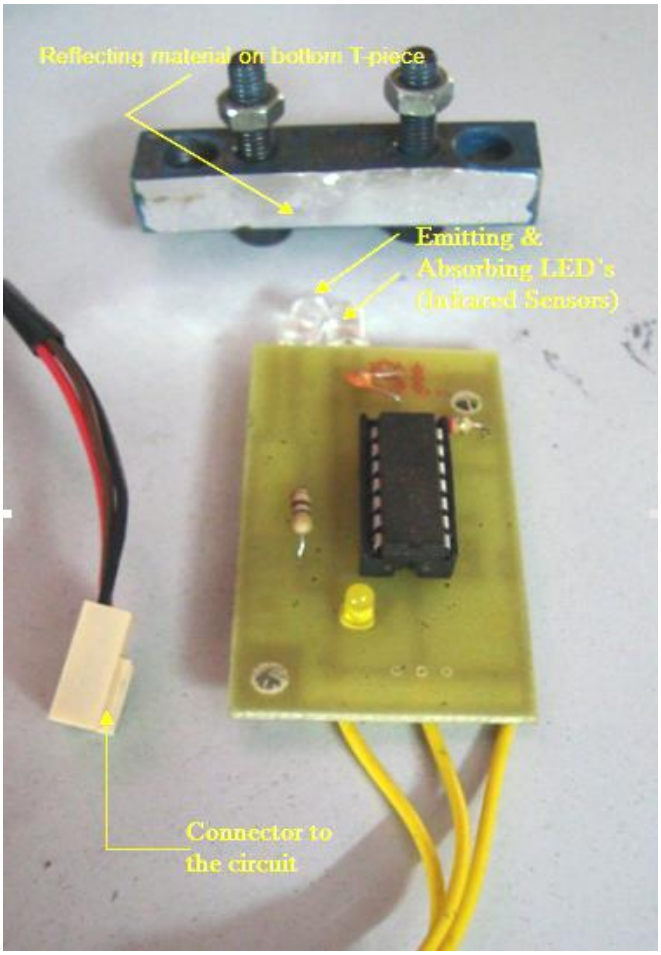

Figure 10 Control and sensor circuit

Failed specimen as well as the eccentric removed. A new eccentric and the specimen were fixed and the machine was started again. Series of experiments were conducted using same procedure to get numbers of experimental data for analysis.

Both ways, experimental as well as software simulation, were used to see the accuracy of resulting datas. Fe-Safe [9], commercially available software was used for the work. Fe-Safe is developed by Safe Technology Limited, formed in 1987. It is one of the world-wide leading suppliers of durability software especially in multiaxial fatigue analysis solutions. Fe-Safe is well-suited for analyzing all aspects of life-prediction of both 2-D and 3-D components under uniaxial or multiaxial loading. The Fe-Safe software also offers the flexibility to interface with multiple finite element analysis software codes like ANSYS [10], ABAQUS etc. Preprocessing is the first step for a fatigue analysis. The steps consist of creating the model and mesh and specifying the material properties, loads, and boundary conditions. Fe-Safe can read FEA data (stresses, strains, and temperatures) from several other third-party software files. ANSYS was chosen for its geometry modeling and high quality meshing capabilities along with the additional benefit that fatigue results can be post-processed directly in ANSYS.

IV. EXPERIMENTAL FEA RESULT AND DISCUSSION

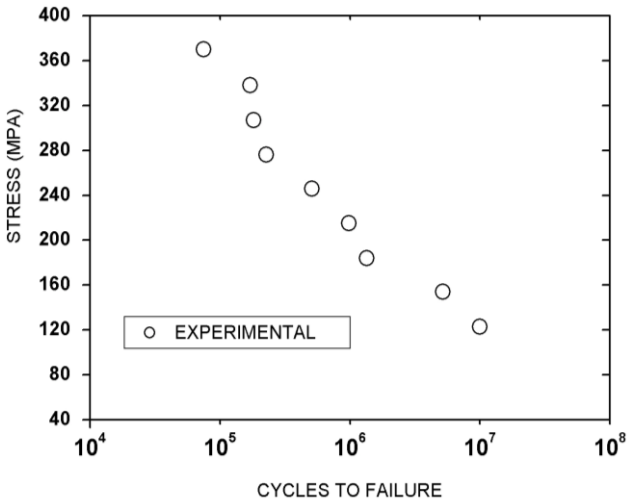

Figure 11 SN Curve from Constant Amplitude Experimental Data

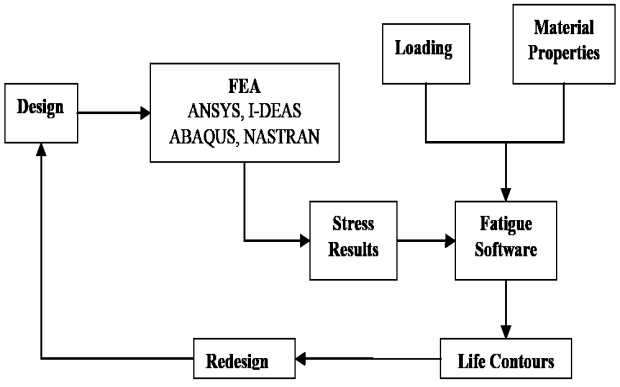

Figure 12 Outlines a FEA – based durability analysis procedure

A. Software simulation analysis

Fe-Safe provides the flexibility of selecting both stress/ strain life methodologies and the choice of a fatigue algorithm based on either uniaxial or biaxial loading. Several simulations were computed using the different fatigue algorithms and data is analyzed from which some of data are represented in this paper. Selectively fatigue failure data of 52421, 128034 and 5123462 are discussed.

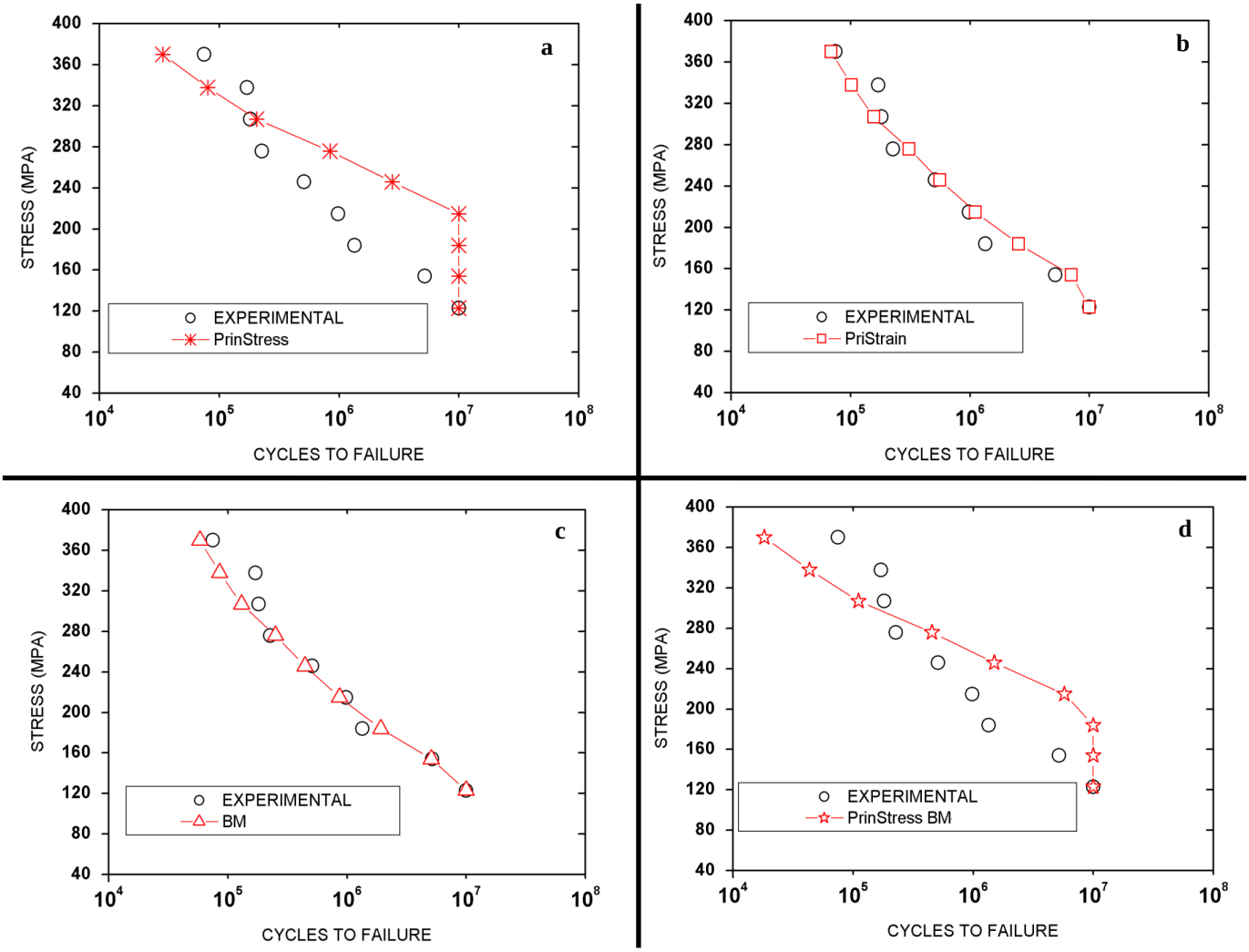

Figure 13 Prediction of fatigue life cycle using simulation of various Fe – Safe algorithm : (a) Principal Strain Algorithm, (b) Brown – Miller Algorithm, (c) Principal Stress Life Algorithm and (d) Brown – Miller Combined Direct and Shear Stress Algorithm.

Figure 13 (a) shows the life prediction utilizing Biaxial Principal Strain for the given material used in this study. It is observed that this approach predicts the fatigue life for low cycles to failure with the best accuracy. For mid-range to a high number of cycles, a higher life is predicted as compared with test results. Draper [11, 12] recommends that a Biaxial Principal Strain approach be used for brittle metals. Figure 13 (b) utilizes a Biaxial Brown-Miller algorithm. It predicts the fatigue life with reasonable accuracy. However, as the number of cycles to failure is increased the predicted fatigue life is greater than the test results. Figure 13 (c) and 13 (d) shows the predicted fatigue life for two different biaxial stress-life algorithms i.e. Principal Stress and Brown – Miller Combined Direct and Shear Stress Algorithm. The stress life methodology does not account for the effects of plasticity and thus significantly under-predicts the fatigue life. Even in this simplest of test cases the stress life approach, while conservative, is not very accurate. An important fact must be noted that within the fatigue community, calculated predicted fatigue lives within an order of 5 is presumed to be reasonable and a calculated life within an order of 2 is considered exceptional [13].

The fatigue crack pattern of three selected wedge shaped steel sample was as shown in figure 15. The failure crack shifted towards the lower cross section area with the number of cycles for failure is increased that is due to shifting of principle stress. This fact can be understood by software simulation. ANSYS software used to shows this fact, refer figure 14 (a, b and c) where red area is highly concentrated zone of principle stress from and serve as origin of fatigue cracks.

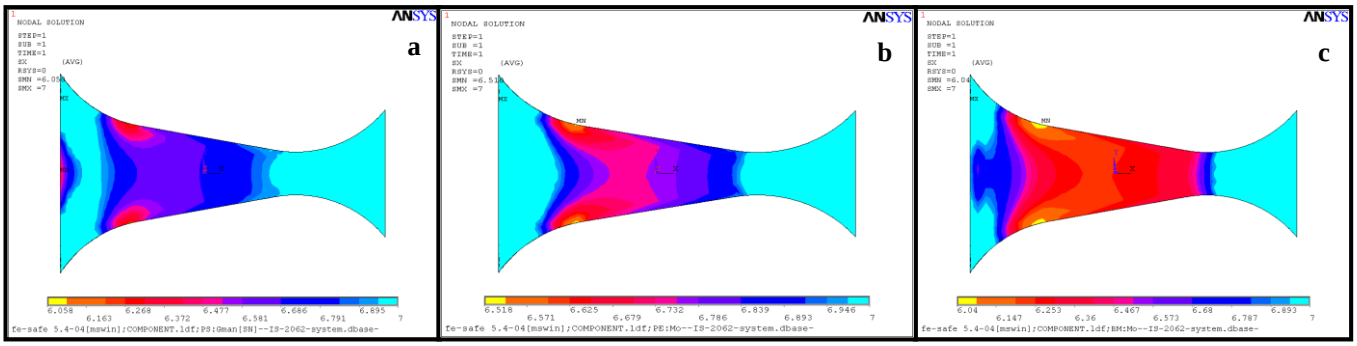

Figure 14 ANSYS software analysis of wedge steel sample for principle stress with respect to total number of fatigue cycle: (a) 52,421, (b) 1,28,034 and (c) 51,23,462.

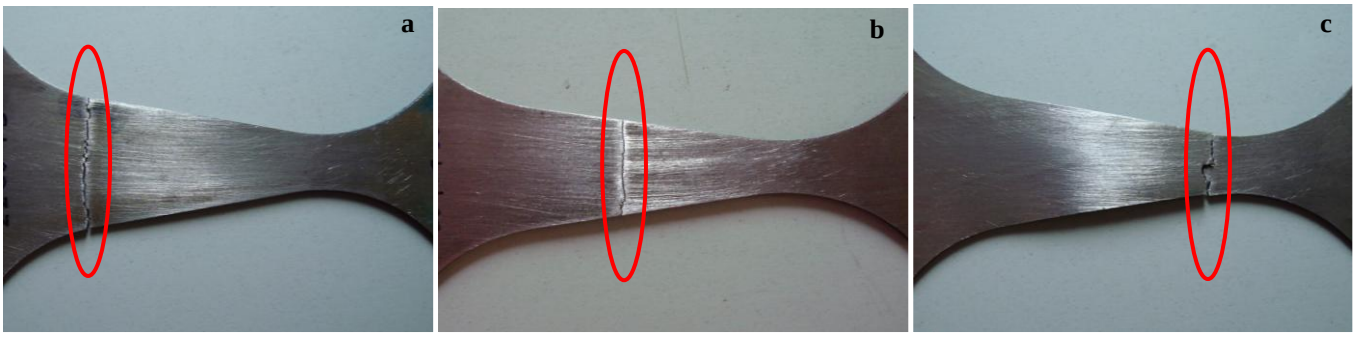

Figure 15 Final fatigue crack pattern with respect to total number of fatigue cycle: (a) 52,421, (b) 1,28,034 and (c) 51,23,462

The fracture analysis was carried out using scanning electron microscope (JEOL 5610 LV) to study the fatigue crack pattern and affect on mode of fracture at micolevel, refer figure 16, 17 and 18.

It is clear from the fractrography images that flatness of failure surface increased with number of fatigue cycle. Hence the cleavage form of failure observed which help to enhance brittle mode of fatigue failure with higher number of fatigue cycles. While lower number of fatigue cycles shows more sheared, rough and dimpled form of failure which is the sign of ductile mode of failure. Centre line (Cheveron mark) appeared on all three fractured surface but more cleared in higher cycle no. without any striation marks which is due to catastrophic failure (high brittleness). Due to higher ductility in lower no. of cycle sample, bulging of structure observed where in some area we can see more dimpled form of failure. Plastic strains are relatively small for longer lives. This can be seen in figure 13, which shows that as the number of cycles increases the strain curve approaches the elastic strain line, resulting in a narrow hysteresis loop. Conversely, for short lives the plastic strain term becomes dominant as compared with the elastic strains. This results in the strain life curve approaching the plastic strain line which is equivalent to an increase in the width of the hysteresis loop. Although a Brown-Miller is typically recommended for ductile materials, the results show that the best approach is dependent on the component geometry and loading. Therefore, the engineer must have a good understanding of the different fatigue algorithms and their application to accurately predict the life of a component.

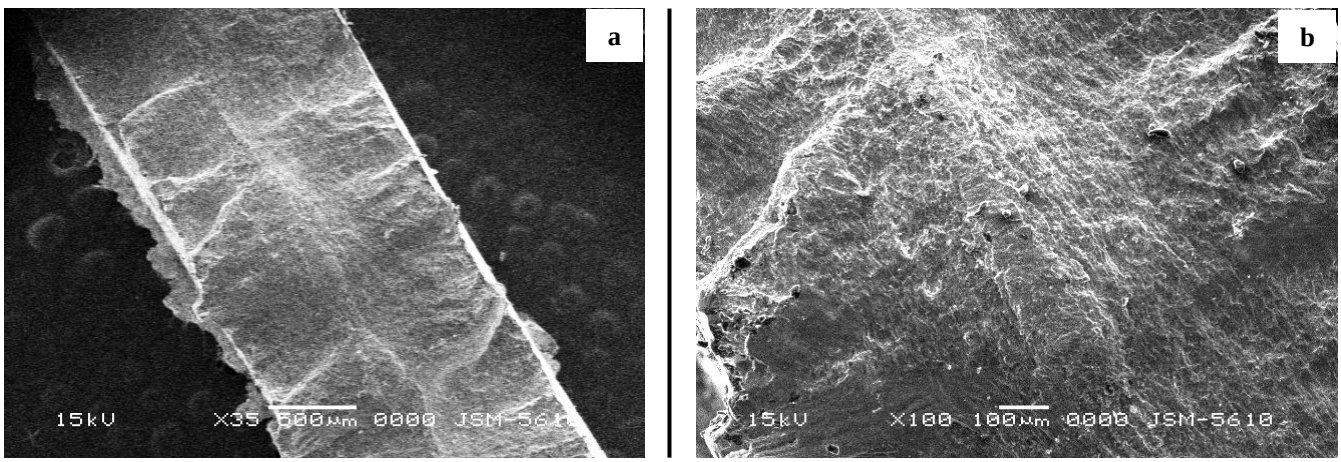

Figure 16 Fractrography image of fatigue sample failed at 52421 numbers of cycles: (a) at 35 X and (b) at 100 X.

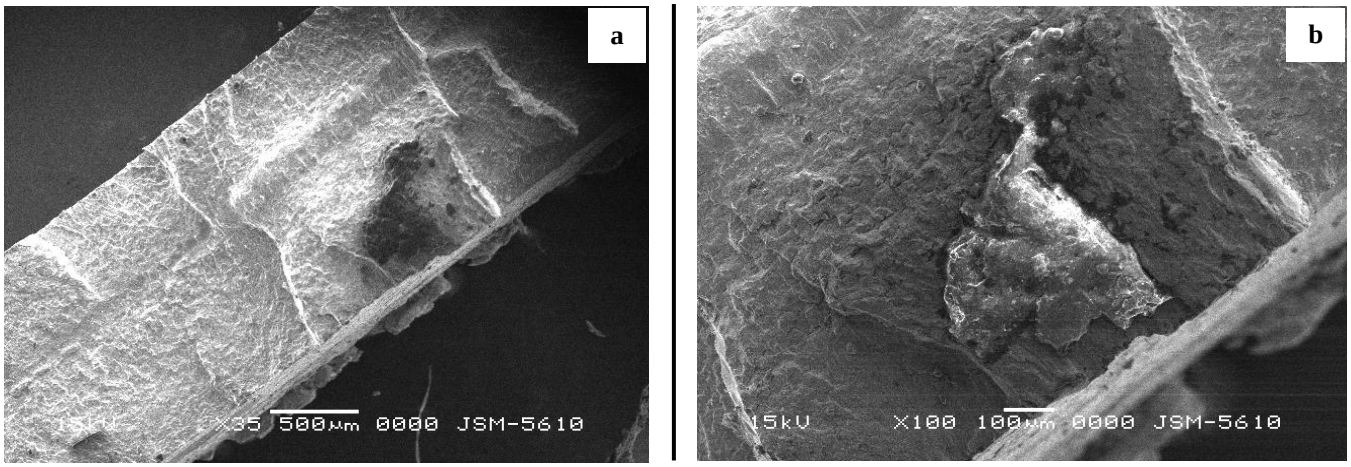

Figure 17 Fractrography image of fatigue sample failed at 128034 numbers of cycles: (a) at 35 X and (b) at 100 X.

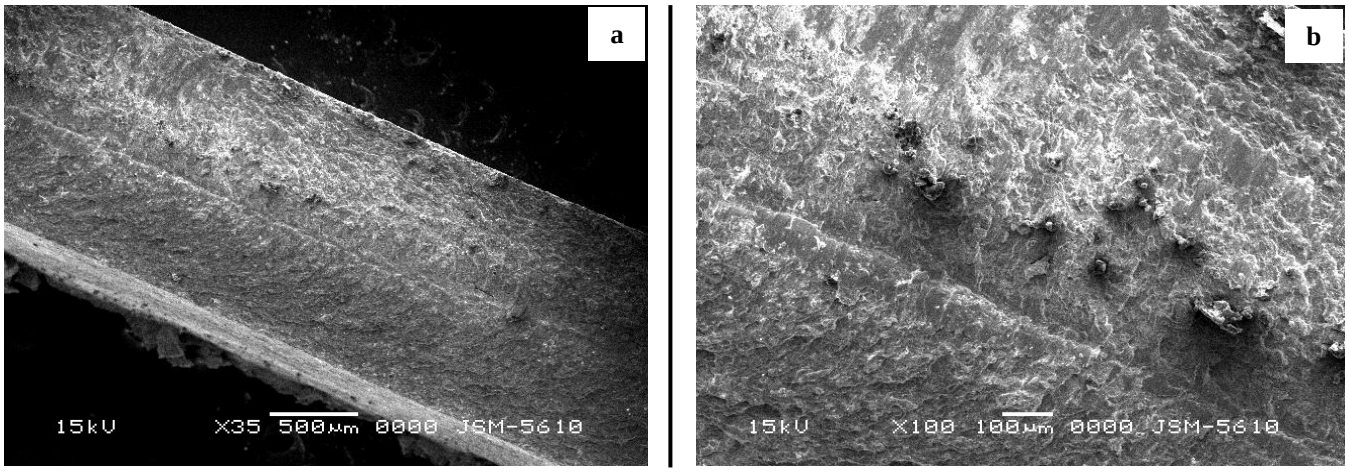

Figure 18 Fractrography image of fatigue sample failed at 51,23,462 number of cycles : (a) at 35 X and (b) at 100 X.

V. CONCLUSION

The main goal of this work was to gain an insight into the available life prediction methodologies and their use. This work has shown that commercially available fatigue software codes, predicted fatigue life with reasonable accuracy and efficiency. This was demonstrated with the predicted fatigue life of the flat sheet metal plate under constant amplitude loading.

Although this is a relatively simple geometry with no published results, it provided insight into the capabilities of current fatigue and durability software. In addition, the computational time was minimal with an analysis time under 30 minutes even when the applied loading consisted of 9 X 4 (36 loading cases).

The numerical simulations for this classical model also helped to reiterate the many pitfalls that may occur when conducting a life prediction analysis. In addition to accurate applied loadings, accurate material properties are essential, as well as the correct use of the stress and strain life algorithms, with and without mean stress correction.

VI. RECOMMENDATION FOR FUTURE WORK

Future work needs to be performed in several key areas. A more detailed understanding of the applied load history as well as an investigation into the capabilities of the fatigue and durability software to incorporate the effects of multiple loads not in phase should be performed.

Use of Spectrum loading can also be taken as a separate effort to gain further understanding into the application areas like automotive and aircraft industries. Investigation under variable amplitude loading will provide further confidence in the use of fatigue and durability software. This type of research can also be taken to the new field of interest like Composite and so on.

REFERENCES

[1] Everett, Richard A. Jr., "A Comparison of Fatigue Life Prediction Methodologies for Rotorcraft," Journal of the American Helicopter Society, Vol. 37, No. 2, pp. 54-60, April 1992.

[2] Everett, Richard A. Jr., Bartlett, Felton D. Jr., Elber, Wolf, "Probabilistic Fatigue Methodology for Safe Retirement Lives," Journal of the American Helicopter Society, Vol. 37, No. 2, pp. 41-53, April 1992.

[3] Newman, J. C. Jr., "Crack Closure Model for Predicting Fatigue Crack- Growth under Aircraft Spectrum Loading," ASTM STP 748, American Society of Testing and Materials, Philadelphia, 1981, pp 53-84.
[4] Newman, J. C. Jr., Phillips, E.P., Swain, M. H., "Fatigue-Life Prediction Methodology using Small-Crack Theory," International Journal of Fatigue, Vol. 21, Issue 2, 1999, pp. 109-119.
[5] Newman, J. C. Jr., Phillips, E. P., Everett, R. A. Jr., "Fatigue Analyses Under Constant Amplitude- and Variable Amplitude Loading Using Small-Crack Theory," NASA/TM-1999-209329, 1999.
[6] Newman, J. C. Jr., Irving, P. E., Lin, J., Le, Dy, "Crack-Growth Predictions in a Complex Helicopter Component Under Spectrum Loading", Proceedings of the 8th Joint FAA/DoD/NASA Conference on Aging Aircraft, Palm Springs, CA, January 2005.
[7] Newman, J.C. Jr., "FASTRAN II – A Fatigue Crack Growth Structural Analysis Program," NASA TM 104159, 1992.
[8] Andresen, P. L. "Corrosion fatigue testing ASM Handbook, Vol. 19 Fatigue and Fracture, Materials Park, ASM International, 1996.
[9] Safe Technology Limited, "fe-safeWorks version 5 – Durability Analysis Suite from Safe Technology," Sheffield UK, 2005. http://www.safetechnology.com
[10] ANSYS, Inc., Modeling Software, ANSYS 11.0 Documentation. http://www.ansys.com
[11] Draper, John, Modern Metal Fatigue Analysis, Safe Technology Limited, Sheffield UK, 2004.
[12] Draper, J., Aveline, R., "How to Achieve Valid Results in Durability Analysis from ANSYS," Proceedings of the ANSYS International User's Conference, Pittsburgh USA, 2004.
[13] Draper, J., Mercer, Ian, Personal Correspondence, February to March 2006, MS thesis "DEVELOPMENT OF A PRACTICAL FATIGUE ANALYSIS METHODOLOGY FOR LIFE PREDICTION OF ROTARY- WING AIRCRAFT COMPONENTS" By Jason Michael Cowell, North

hnp.15.met@gmail.com *Corresponding author Email Id